Analysis of the 40 meter radiotelescope beam and aperture efficiency at 100 GHz from measured data

José A. López-Pérez
Pablo de Vicente

May, 2012

Informe IT-OAN-2012-12

Change Record

Version	Date	Author	Comments
1.0	09.03.2012	J.A. López-Pérez	First version
2.0	16.05.2012	J.A. López-Pérez	Second version

Contents

List of Figures

List of Tables

1 Introduction

This report shows the results of the 40 meter radiotelescope beam analysis at 100 GHz, performed with real data acquired with observations of planet Mars. Some issues, like a beam broader than expected and a coma sidelobe are revealed.

In addition, the aperture efficiency budget is shown and the different efficiency factors are evaluated in order to check the agreement between the aperture efficiency estimated with holography measurements and the one computed by radiometric means.

2 Theoretical approach

2.1 Illumination efficiency of a circular aperture with gaussian fied distribution

Let us consider the 40 meter main reflector circular aperture illuminated by an electromagnetic field whose amplitude distribution is gaussian, according to the following law:

$$E(r) = e^{\alpha \cdot r^2} \tag{1}$$

where $E(r)$ is the aperture field, r is the normalized aperture radius and α is a parameter related with the taper of the field at the rim of the reflector through the following equation [1]:

$$\alpha = \frac{T}{20} \cdot \ln(\frac{1}{10}) \tag{2}$$

For $T = -12dB$ we have $\alpha = 1.3816$. Table 1 shows the value of α for some other taper values.

The illumination efficiency is given by the following formula [1]:

$$\eta_i = \frac{[\int_A E(r) \cdot \mathrm{d}A]^2}{\int_A |E(r)|^2 \cdot \mathrm{d}A} \tag{3}$$

where A is the geometrical aperture of the reflector.

The substitution of equation 1 into 3 yields [1]:

$$\eta_i = \frac{2(1 - e^{-\alpha})^2}{\alpha(1 - e^{-2\alpha})} \tag{4}$$

Table 1 gives the values of illumination efficiency for each taper, too.

Taper (dB)	**Parameter** α	**Efficiency** η_i
-10	1.1513	0.90
-12	1.3816	0.87
-15	1.7269	0.81
-20	2.3026	0.71
-25	2.8782	0.62
-30	3.4539	0.54
-35	4.0295	0.48

Table 1: Value of parameter α and illumination efficiency versus taper for a gaussian aperture field.

Assuming a constant aperture phase distribution of the field and a rotationally symmetric amplitude distribution, as for the gaussian one given in equation 1, the normalised radiation pattern can be written as [1]:

$$F(u) = \frac{\pi D^2}{2} \cdot \int_0^1 E(r) \cdot J_0(ur) \cdot r \, \mathrm{d}r \tag{5}$$

where $J_0(ur)$ is the Bessel function of first kind and order zero, r is the normalised aperture radius and u is given by $u = \frac{\pi D}{\lambda} \sin\theta$, being D the diameter of the aperture, λ the wavelength and θ the angular coordinate.

The computation of the power pattern (square of $F(u)$) is performed numerically for different values of the taper. The results of this computation are shown in figure 1.

With the help of this computation, the half-power beam-widths (HPBW) of these patterns at 100 GHz are obtained for each taper value. The results are summarized in table 2, where it can be seen that the HPBW value is very sensitive on the taper parameter.

In addition, assuming that $\sin\theta \simeq \theta$, which is a good approximation for very narrow beams as in the 40 meter atenna, the HBPBW can be expressed as a function of the ratio $\frac{\lambda}{D}$ as:

$$HPBW = \frac{2 \cdot u_{-3dB}}{\pi} \cdot \frac{\lambda}{D} = b \cdot \frac{\lambda}{D} \tag{6}$$

being b a constant, whose values are given in table 2, too, and being u_{-3dB} the value of u at the point $-3dB$ of the normalised power pattern.

The relation among taper and HPBW at 100 GHz can be fitted by a linear function whose expression is the following:

$$HPBW('') = -0.248 \cdot T_{dB} + 15.144 \tag{7}$$

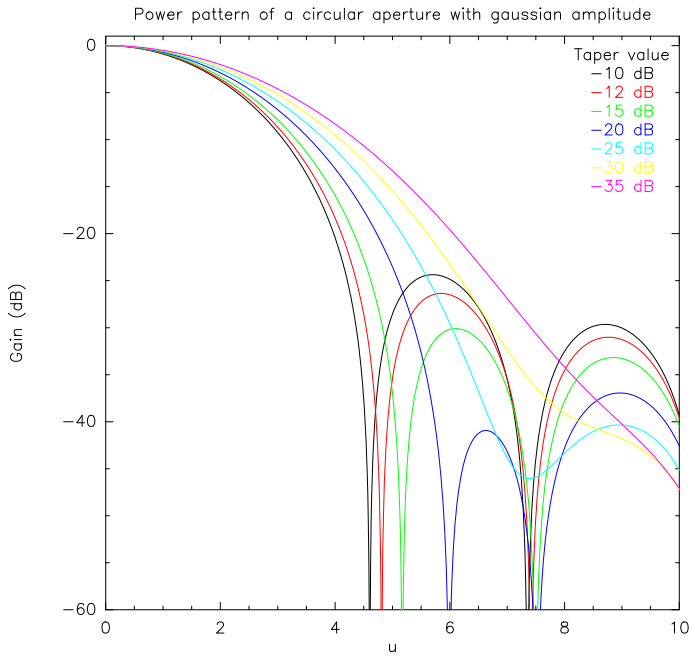

Figure 1: Power pattern of circular aperture with gaussian illumination.

Taper (dB)	u_{-3dB}	**HPBW (″) @ 100 GHz**	**Parameter b**
-10	1.80	17.7	1.1473
-12	1.84	18.2	1.1756
-15	1.91	18.8	1.2160
-20	2.03	19.9	1.2928
-25	2.16	21.2	1.3737
-30	2.29	22.6	1.4626
-35	2.43	23.9	1.5475

Table 2: Value of HPBW @ 100 GHz versus taper for a gaussian aperture field.

2.2 Illumination efficiency of an axially defocused circular aperture with gaussian fied distribution

If the antenna is axially defocused by an amount δ, then the far field pattern will be given by the following equation [1]:

$$F(u) = \int_0^1 E(r) \cdot J_0(ur) \cdot e^{-j\Delta\Phi(r)} \cdot r \, \mathrm{d}r \tag{8}$$

where $\Delta\Phi(r)$ is the defocused phase term:

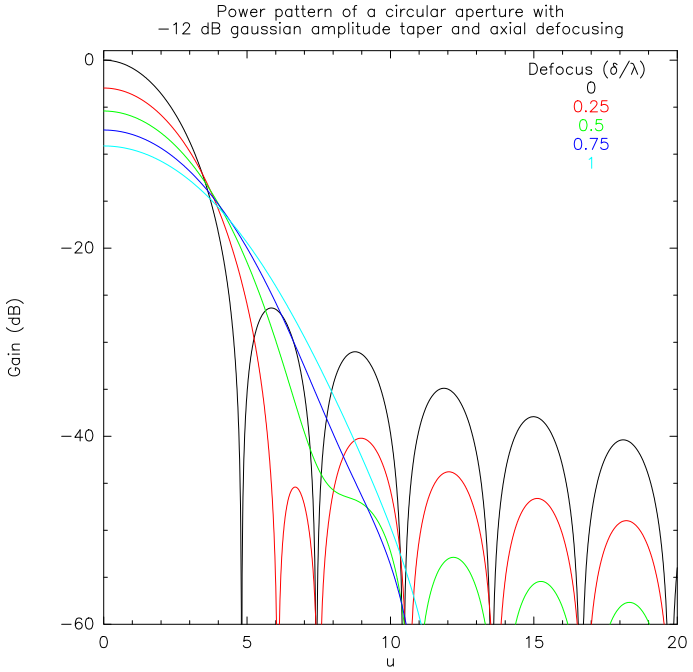

Figure 2: Power pattern of circular aperture with -12 dB gaussian amplitude taper and axial defocusing.

$$\Delta\Phi(r) = \frac{2\pi\delta}{\lambda} \cdot (1 - \cos\Psi_0) \cdot r^2 = \beta \cdot r^2 \tag{9}$$

being Ψ_0 the subtended half-angle of the main reflector and β a factor to incorporate all the factors in front of r^2.

Equation 8 has been numerically computed too, in order to evaluate the beam broadening and gain loss of a -12 dB gaussian tapered circular aperture as a function of the axial displacement.

Figure 2 shows the normalised power patterns (with respect to the focused case) of such an aperture for different values of the ratio $\frac{\delta}{\lambda}$ from 0 to 1 in 0.25 steps.

From these computations, the HPBW at 100 GHz and the gain loss in the defocused case are derived and collected in table 3. It can be seen that an axial defocussing of one wavelength implies a HPBW broadening from 18.2″ to 26.8″.

Axial defocus ($\frac{\delta}{\lambda}$)	u_{-3dB}	**HPBW** ($''$) **@ 100 GHz**	**Gain loss (dB)**
0.00	1.84	18.2	0.0
0.25	2.04	20.1	-2.97
0.50	2.26	22.3	-5.41
0.75	2.49	24.6	-7.43
1.00	2.71	26.8	-9.12

Table 3: Value of HPBW @ 100 GHz and gain loss versus axial defocusing for a -12 dB gaussian taper aperture field.

2.3 Illumination efficiency of a laterally defocused circular aperture with gaussian fied distribution

Under construction ...

3 Beam convolution with planetary disk

In this section the gaussian beam pattern, computed in the previous section, is going to be convolved with the power distribution of the planet to be used in the observations (Mars). For the sake of simplicity, planet Mars is going to be considered as a $13.8''$ disk, because that was its apparent size during the epoch of the measurements, with uniform power flux.

Figure 3 shows the result of the convolution process. Assuming a -12 dB taper, the antenna HPBW is $18.2''$, according to table 2. When convolved with a planetary disk of $13.8''$, the resulting beam will have a HPBW of $20.5''$. This is the HPBW that must be measured with either pointing cross-scans or raster maps. However, the measured HPBW is broader, as will be shown in section 4.

According to [1], the resulting HPBW from the convolution of a planetary disk and a radiotelescope beam, can be approximated by the following equation:

$$\theta_{conv} = \sqrt{{\theta_b}^2 + \frac{\ln 2}{2}{\theta_s}^2} \tag{10}$$

where θ_{conv} is the convolved HPBW, θ_b is the HPBW of the radiotelescope and θ_s is the angular size of the disk.

Assuming $\theta_s = 13.8''$, the convolved HPBW as a function of the amplitude taper is given in table 4.

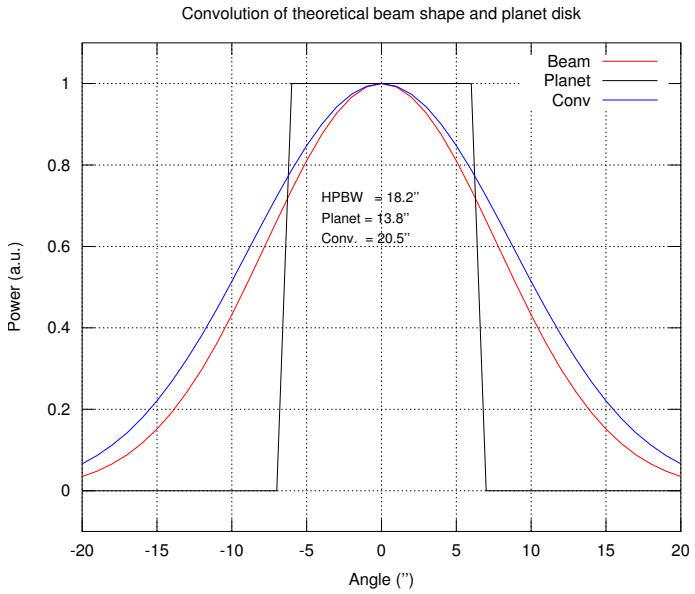

Figure 3: Result of convolution of antenna beam and planet.

Taper (dB)	**HPBW** $\theta_b('')$	**Convolved HPBW** $\theta_{conv}('')$	**Difference** $\theta_{conv} - \theta_b$
-10	17.7	19.5	1.8
-12	18.2	19.9	1.7
-15	18.8	20.5	1.7
-20	19.9	21.5	1.6
-25	21.2	22.7	1.5
-30	22.6	24.0	1.4
-35	23.9	25.2	1.3

Table 4: Value of convolved HPBW @ 100 GHz versus taper for a gaussian aperture field.

4 Half-Power Beam-Width measurements and beam deconvolution

Measurements of the convolved HPBW have been performed by pointing scans across Mars, Venus and Saturn. Figure 4 shows the values of the HPBW derived from these cross-scans in both axes (azimuth and elevation).

From figure 4, an average value of $24''$ for the convolved HPBW can be estimated, although the data dispersion is noticeable at both edges of the plotted elevation range. An average value for all the elevation range has

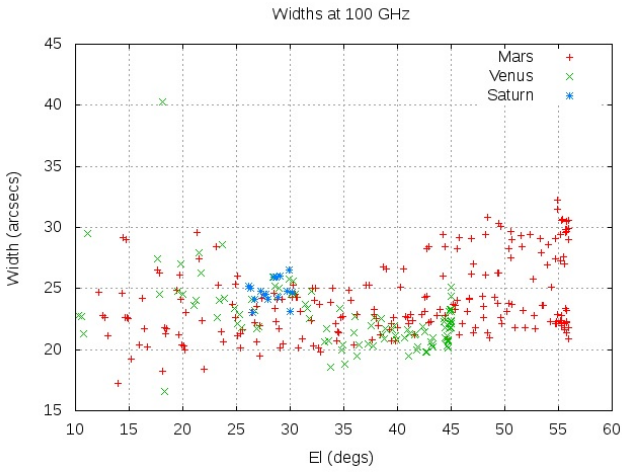

Figure 4: Convolved HPBW measurements at 100 GHz.

been considered for the sake of simplicity in the following discussion.

If a convolved HPBW of 24″ is assumed, then the deconvolved beam will be 22.6″ which would correspond to a gaussian taper of -30 dB, according to table 4 and, therefore, to an illumination efficiency of $\eta_i = 0.543$, according to table 1.

This derived gaussian taper of -30 dB is not realistic, as it is much higher than the nominal -12 dB, so one hypothesis to explain the beam broadening is to think that it is due to a subreflector axial defocussing rather than due to an strong taper.

For a -12 dB taper, the corresponding HPBW is 18.2″, but this HPBW would increase to the deconvolved HPBW of 22.6″ if an axial defocus in the range 0.5λ to 0.75λ (i.e., 1.5 to 2.25 mm) would be present, according to table 3. However, all the measurements were performed with a previous subreflector axial focus calibration. Therefore, this hypothesis can be discarded.

Another hypothesis to explain the broadening is a lateral offset in subreflector position, which wasn't optimized neither in X nor Y axis during these measurements. This hypothesis will be discussed in section 5.

5 Beam maps using Mars

Figure 5 shows the measured beam shape using on-the-fly (OTF) raster scans over planet Mars at four different elevation angles (31°, 40°, 47° and 58°). The maps are plotted in a normalised scale in decibels and the contour levels are given from -3 dB to -12 dB in 3 dB steps.

From this figure, a coma sidelobe can be clearly seen, particularly at 31° and 40° elevation, and it is less pronounced at the other two elevation angles. The position of this coma lobe is 40″ north of the main lobe, approximately.

It has to be remembered again that no subreflector position optimization for the 3 mm receiver was performed (except in axial direction) after the holography adjustments, and the astronomical observations were performed considering the 22 GHz receiver pointing model and its corresponding subreflector position look-up table.

The presence of the coma sidelobe implies the existence of a subreflector lateral defocussing, which will be causing both a beam broadening and an additional reduction in antenna efficiency.

From the results of these maps, it was verified that a +6 mm offset in Y axis of the subreflector reduced the coma sidelobe significantly, as shown in section 10 of [2].

The efficiency reduction due to this coma lobe is about 0.8 and it can be estimated from figure 14 in [2] by comparison of the scan peak values at y = 0 mm (15 Kelvin) and y = +6 mm (18.6 Kelvin).

In addition, from this figure with data at 85 GHz, the deconvolved HPBW's at 100 GHz for y = 0 mm and y = +6 mm can be obtained. These values are 21.4″ and 18.4″, respectively. This result shows the beam broadening due to the lateral defocussing.

The corresponding taper value for the HPBW with y = +6 mm is -13.1 dB, which is close to the nominal one (-12 dB), and it drives to an illumination efficiency of 0.84.

The HPBW computed from the maps on Mars is 28″, approximately. This implies that the deconvolved HPBW for the antenna is 26.4″, which is even broader than the value derived in section 4 (22.6″) and from figure 14 in [2] (21.4″). This is an additional result which shows a new confirmation of the beam broadening.

Once more, this broadening is not caused by a subreflector axial defocus as the maps were acquired after a previous axial focus calibration of the subreflector.

These results demonstrate that an optimization for the subreflector position in all its degrees of freedom (X, Y, Z, X-tilt, Y-tilt) for the 3 mm receiver is mandatory, in order to obtain the maximum aperture efficiency of the full

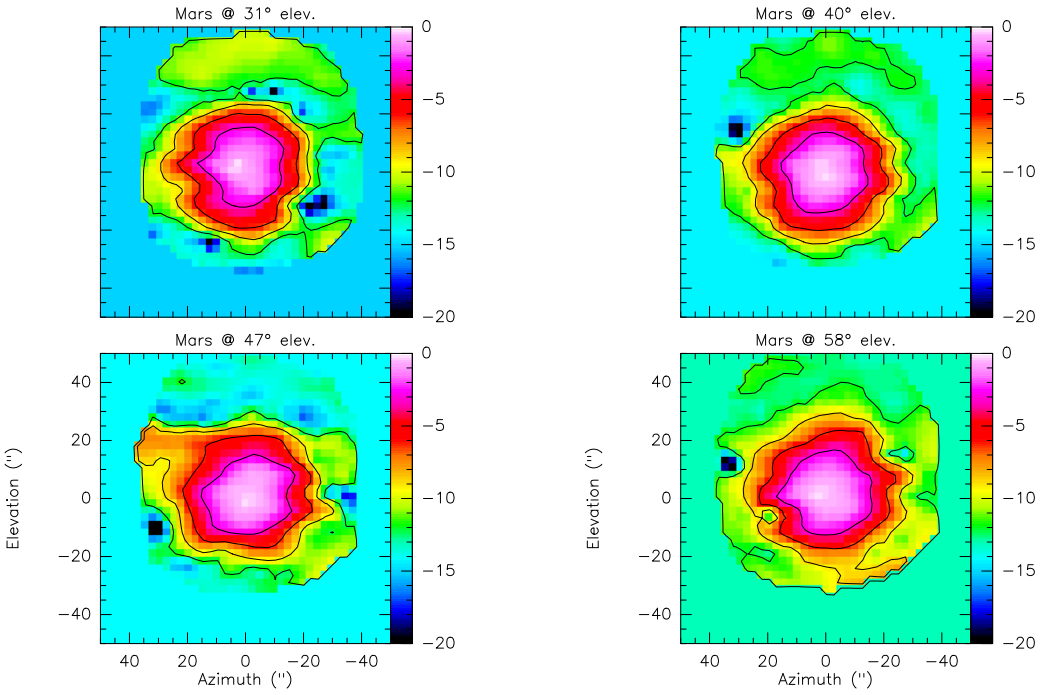

Figure 5: Measured beam maps on planet Mars.

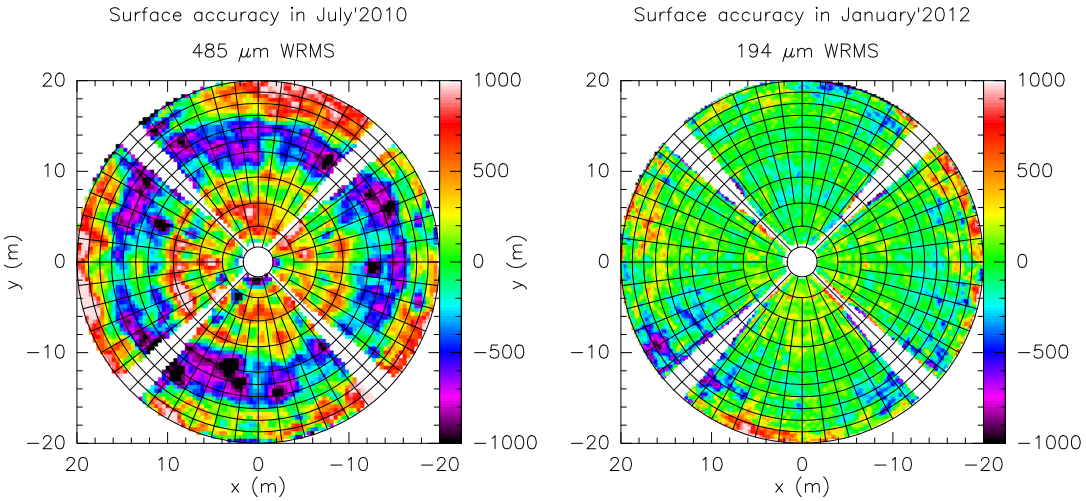

Figure 6: Holography surface accuracy improvement (scale in microns).

optical system. However, it might be evaluated if it is worth to carry out this task before the final holography surface adjustment.

Mirror nr.	**Surface Accuracy (μm RMS)**	**Surface Tol. Eff. @ 86 GHz**	**Surface Tol. Eff. @ 100 GHz**
M1	**194**	0.613	0.516
M2	50	0.968	0.957
M3	25	0.992	0.989
M4	25	0.992	0.989
M5	40	0.979	0.972
M6	7	0.999	0.999
M7	7	0.999	0.999
M8	17	0.996	0.995
M9	17	0.996	0.995
Total	**209**	**0.567**	**0.464**

Table 5: Surface accuracy and efficiency for the mirrors of the 3-mm receiver path.

6 Aperture efficiency budget

In this section, the aperture efficiency budget is shown. It includes all the terms with a relevant impact on the aperture efficiency of the radiotelescope.

Table 5 shows the contribution to the overal surface accuracy of each reflecting surface in the path of the 3 mm receiver. The value for M1 surface accuracy is derived from radio-holography measurements (see figure 6). For the remaining mirrors, their manufacturing accuracy value has been used. Their corresponding surface tolerance efficiency has been computed according to the Ruze formula [3] at both 86 and 100 GHz.

The factors included in the aperture efficiency are shown in table 6, where the taper efficiency value comes from the results of section 4, assuming a -13.1 dB amplitude taper; the reduction in efficiency due to the coma lobe is got from section 5; the spillover efficiency is assumed to be 0.9, as considered in the design; the blockage efficiency is taken from the computations shown in [4]; the surface tolerance efficiency comes from table 5 and the insertion losses of the vertex membrane and the $\frac{\lambda}{4}$ polarizer plate were taken from [2] and are assumed to be the same at both frequencies.

The final values for the estimated aperture efficiency are 28% @ 86 GHz and 23% @ 100 GHz. These values have to be compared with the ones determined in [2] by radiometric measurements at 86 GHz and 100 GHz, which are 21% and 12.5%, respectively.

The origin of these differences has to be investigated.

In addition, the aperture efficiency estimated by the holography data

reduction software, from prime focus position with an illumination equal to the one produced by the holography receiver test feed (gaussian -11 dB taper), is 38% at 86 GHz.

In order to compare this value with the previous ones, this efficiency has to be reduced by the efficiency factors due to mirrors M2 to M9, the blockage, the membrane, the polarizer and the coma. Then, the resulting aperture efficiency is 23%, which is in between the two values mentioned above.

Finally, if the subreflector position is optimized, the aperture efficiency will raise up to 36% at 86 GHz and 29% at 100 GHz. These values are obtained from table 6 when coma efficiency is set to 1.0.

Efficiency factor	**Value @ 86 GHz**	**Value @ 100 GHz**
Taper	0.84	0.84
Coma	0.8	0.8
Spillover	0.9	0.9
Blockage	0.92	0.92
Surface tolerance	0.567	0.464
Vertex membrane	0.94	0.94
Polarizer plate	0.96	0.96
Total	**0.28**	**0.23**

Table 6: Aperture efficiency budget.

7 Conclusions

The results of this report can be summarized in the following conclusions:

- The radiotelescope HPBW is broader than expected, according to the results shown in section 4. The reason seems to be a lateral offset in the position of the subreflector. The beam broadening is revealed in [2], too.
- The beam pattern suffers from a coma sidelobe, according to figure 5, which reduces the overall aperture efficiency by a factor 0.8. It has been verified that this coma lobe is due to a lateral subreflector offset. As a result, an optimization of the subreflector position for the 3 mm receiver is mandatory in order to get the maximum aperture efficiency. When the subreflector offset in Y direction is corrected, the beam narrows from 21.4″ to 18.4″, whose corresponding taper is -13.1 dB, which is close to the nominal one.
- The holography measurements return a surface accuracy of 194 μm RMS. The aperture efficiency estimated from holography is 23% at 86 GHz and it is inside the range of efficiencies computed by radiometric means in [2] (21%) and in the analysis performed in this report (28%).
- A discrepancy between the efficiency values at 100 GHz exists and has to be investigated.
- The main reflector surface accuracy computed in [2] (270 μm RMS) is 40% higher that the holography measurement (194 μm RMS). This is because the gain reduction due to the subreflector lateral defocussing is not considered. In fact, the difference decreases to 11% (215 μm RMS) when it is considered.
- The maximum achievable aperture efficiency is estimated to be 36% at 86 GHz and 29% at 100 GHz from the 3mm receiver position.

Acknowledgments

The authors wish to acknowledge the help provided by Tim Finn with some numerical computations of the beam patterns.

References

[1] J. W. M. Baars, *The Paraboloidal Reflector Antenna in Radioastronomy and Communication: Theory and Practice*, vol. 348 of *Astrophysics and Space Science Library*. Springer, 2007.

[2] P. de Vicente, "The 40m radiotelescope at the 87 - 110 GHz band after holography," Tech. Rep. Informe Técnico IT-OAN 2012-09, Centro Astronómico de Yebes, 2012.

[3] J. Ruze, "Antenna Tolerance Theory - A Review," *Proc. IEEE.*, vol. 54, no. 4. Apr., pp. 633–640, 1966.

[4] P. de Vicente, "Eficiencia por bloqueo en un paraboloide. Antena de 40 m.," Tech. Rep. Informe Técnico CAY 1998-10, Observatorio Astronómico Nacional, 1998.